JOURNAL OF CHEMOMETRICS
*J. Chemometrics* **13,** 95–110 (1999)

# APPLICATIONS AND NEW DEVELOPMENTS OF THE DIRECT EXPONENTIAL CURVE RESOLUTION ALGORITHM (DECRA). EXAMPLES OF SPECTRA AND MAGNETIC RESONANCE IMAGES

WILLEM WINDIG,[1]* BRIAN ANTALEK,[1] LOUIS J. SORRIERO,[1] SABINA BIJLSMA,[2] D. J. LOUWERSE (AD)[2] AND AGE K. SMILDE[2]

[1]*Imaging Research and Advanced Development, Eastman Kodak Company, Rochester, NY 14650-2132, USA*

[2]*Process Analysis and Chemometrics, Department of Chemical Engineering, University of Amsterdam, The Netherlands*

SUMMARY

Recently, a new multivariate analysis tool was developed to resolve mixture data sets, where the contributions ('concentrations') have an exponential profile. The new approach is called DECRA (direct exponential curve resolution algorithm). DECRA is based on the generalized rank annihilation method (GRAM). Examples will be given of resolving nuclear magnetic resonance spectra resulting from a diffusion experiment, spectra in the ultraviolet/visible region of a reaction and magnetic resonance images of the human brain. Copyright © 1999 John Wiley & Sons, Ltd.

KEY WORDS: generalized rank annihilation method (GRAM); nuclear magnetic resonance (NMR); UV-vis; magnetic resonance imaging (MRI); exponential; chemometrics

## 1. INTRODUCTION

### 1.1. Self-modeling mixture analysis

Given a data set with mixture spectra, the task of self-modeling mixture analysis is to determine mathematically the spectra of the pure contributions ('concentrations') in the original spectra without using reference data.

In a recent tutorial-like paper the principles of self-modeling mixture analysis have been explained avoiding mathematical details.[1] A shortened version of this explanation will be given in this paper. For a more detailed review see Reference 2.

A simulated mixture is created by combining the two spectra of pure components labeled in Figure 1 as **spectrum 1** and **spectrum 2**. The mixture data set presented as **mixture 1, mixture 2** and **mixture 3** is created by using the contributions listed in Figure 1. The task of self-modeling mixture analysis is the following: given *only* **mixture 1**, **mixture 2** and **mixture 3**, calculate the pure spectra and their contributions.

* Correspondence to: W. Windig, Imaging Research and Advanced Development, Eastman Kodak Company, Rochester, NY 14650-2132, USA.

CCC 0886–9383/99/020095–16 $17.50

*Received 4 September 1998*
*Accepted 20 November 1998*

| | spectrum 1 | spectrum 2 | spectrum 3 | spectrum 4 |
|---|---|---|---|---|
| mixture 1 | 1 | 0.50 | 0.93 | 0.27 |
| mixture 2 | 1 | 1 | 0.80 | 0.80 |
| mixture 3 | 0.50 | 1 | 0.27 | 0.93 |
| mixture 4 | 1 | 0.25 | 1 | 0 |
| mixture 5 | 1 | 0.50 | 0.93 | 0.27 |
| mixture 6 | 0.50 | 0.50 | 0.40 | 0.40 |

Figure 1. Diagram representing principle of self-modeling mixture analysis (reprinted from Reference 1, with permission from Elsevier Science)

Next to the solution given by **spectrum 1** and **spectrum 2**, it is also possible to express the mixture data with pure **spectrum 3** and **spectrum 4** with the contributions listed in Figure 1. As a matter of fact, an infinite number of solutions are possible to resolve **mixture 1, mixture 2** and **mixture 3** into pure component spectra and their contributions. The question now is how to find the right 'chemical' solution from the infinite number of 'mathematical' solutions. All the solutions given in Figure 1 can be transformed into each other by simple mathematical means:

$$A = CP \tag{1}$$

In this equation, $A$ represents the mixture data set with the spectra in the rows, $C$ represents the concentration matrix with the concentrations in the columns and $P$ represents the matrix with the pure spectra in the rows. For a data set with ten mixtures of three components where each spectrum contains 100 data points (e.g. wavenumbers), the dimensions of the matrices are $10 \times 100$ for $A$, $10 \times 3$ for $C$ and $3 \times 100$ for $P$.

In order to transform to other results, a transformation matrix needs to be used. If one knows the transformation matrix for the spectra, for example, the transformation matrix for the concentrations is simply its inverse:

$$D = CT^{-1}TP \tag{2}$$

The transformation matrix is obtained by using constraints that result in data with desirable chemical properties such as positivity of spectra and concentrations, unique peaks for the pure components, unimodal character of concentration profiles, etc.

The first step in most self-modeling mixture analyses is to use principal component analysis (PCA)

 

as a starting solution (the 'abstract' solution), which is then transformed into a 'basic' solution using proper constraints, using equation (2) given above.

The use of PCA for chemical applications has been described in the pioneering book *Factor Analysis in Chemistry* by Malinowski and Howery.[3] A major problem is to determine the number of components in a mixture data set, for which Malinowski developed several generally accepted diagnostic techniques.[3–5]

One of the most powerful techniques for transforming the abstract solution into a basic solution is the pure variable technique, which assumes that every pure component has a unique peak. This constraint results in the solution of **spectrum 1** and **spectrum 2** in Figure 1. The pure variable concept originated from the pioneering work of Lawton and Sylvestre[6] and Knorr and Futrell.[7] The pure variable concept was limited to two components until Malinowski extended the technique toward any number of components, using a determinant-based approach.[8,9] The use of the determinant has also been adapted to self-modeling mixture analysis techniques that do not use PCA.[10,11]

Other self-modeling mixture analysis techniques use target factor analysis, developed by Malinowski and Howery.[3] in order to determine the basic solution. For example, Gemperline[12,13] and Vandeginste *et al.*[14] independently developed iterative target factor analysis (ITTFA) to resolve data with unimodal concentration profiles.

Another group of self-modeling techniques apply PCA multiple times. Maeder and co-workers[15,16] developed evolving factor analysis (EFA). By analyzing a time-resolved data set in a forward way (PCA on first two spectra, first three spectra, etc.) and a backward way (last two spectra, last three spectra, etc.), plots of the eigenvalues indicate regions where components are present. This information is then used to resolve the spectra. Malinowski analyzes a data set multiple times by using windows of different sizes in order to determine the regions where components are present. His window factor analysis (WFA) approach avoids some of the problems of EFA.[17,18]

### 1.2. Self-modeling mixture analysis by the three-way method

Although the use of constraints resulted in powerful tools to resolve mixtures of unknown composition, the constraints are generally on a simplification of actual behavior, which leaves ambiguities in the solution. Furthermore, under certain constraints a range of solutions is possible. For example, the solutions given in Figure 1 in the form of **spectrum 1/spectrum 2** and **spectrum 3/ spectrum 4** are both valid solutions using positivity constraints. It is possible, however, to obtain a unique solution from *two* data sets which have a proportional relationship.[19–24] In Figure 1 a second mixture data set is presented as **mixture 4, mixture 5** and **mixture 6**, which has a proportional relation with the data set presented by **mixture 1, mixture 2** and **mixture 3:** the contributions of **spectrum 1** in the second mixture data set are proportional to the contributions of **spectrum 1** in the first mixture data set with a ratio between the contributions of one. The contributions of **spectrum 2** in the second mixture data set are proportional to the contributions of **spectrum 2** in the first mixture data set with a ratio of 0·5.

The equation for a data set proportional to the one in equation (1) is

$$B = C\alpha P \tag{3}$$

The diagonal matrix $\alpha$ contains the proportionality factors. For the two data sets in Figure 1 the diagonal elements of $\alpha$ are 1·00 and 0·50.

As with the first mixture data set, there are an infinite number of solutions possible to resolve the second data set. However, if the two data sets have a proportional relation, *only* the correct solution

 

Table 1. Model for data set *D* with exponential decays, and how it can be split into proportional data sets *A* and *B*

| *D* | | *A* | | *B* | |
|---|---|---|---|---|---|
| Component 1 | Component 2 | Component 1 | Component 2 | Component 1 | Component 2 |
| 27 | 8 | 27 | 8 | 9 | 4 |
| 9 | 4 | 9 | 4 | 3 | 2 |
| 3 | 2 | 3 | 2 | 1 | 1 |
| 1 | 1 | | | | |

will show the proportionality. This is demonstrated in Figure 1. The proper solution of the two mixtures with pure **spectrum 1** and **spectrum 2** shows the proportionality, but the solution with pure **spectrum 3** and **spectrum 4** does not show the proportional behavior of the resolved contributions. It can be proven mathematically that the proportionality is only preserved in one solution. As a consequence, when two proportional data sets are available, resolving them simultaneously with the restriction that the resolved contributions must be proportional will lead to the correct solution. This problem can be solved as the generalized eigenproblem.[22]

When a single spectral data set is analyzed, each spectrum is stored as a vector. A set of spectra are stored in a matrix, where each row represents a spectrum. A vector is a one-way array and a matrix is a two-way array. When two spectral mixtures are analyzed, the data are present in two matrices that form a 'box' of data, called a three-way array. As a consequence, the methods to resolve several data sets simultaneously are called three-way methods.[25]

### 1.3. Resolving mixture data with exponentially decaying contribution profiles

Using pulsed gradient spin echo (PGSE) nuclear magnetic resonance (NMR) spectroscopy, it is possible to generate a series of spectra of mixtures where the contribution of each of the components decays with an exponential profile.[26] The decay of the exponential is a function of the diffusion coefficient of the component. It is possible to generate two proportional data sets from such a data set; see Table 1. Under *D*, two exponential decays are listed. This is representative for the contribution profiles of a data set containing two components. As a next step, *D* will be split into two parts: *A* contains the first three rows of *D*, and *B* contains the last three rows of *D*. The data sets *A* and *B* are proportional. The proportionality factors (matrix $\alpha$ in equation (3)) are 1/3 and 1/2. As a consequence, when a data set is available in which the components have contribution profiles of an exponential character, the data set can be split into two data sets with a proportional character and can thus be resolved unambiguously.

Resolving of exponential data has been described before by Stilbs *et al.*[27] as CORE (component-resolved NMR spectroscopy). The method is based on an optimization routine to resolve the linear combinations of exponentials. This optimization can be time-consuming, e.g. 1 h for four exponentials and 1000 frequency channels. DECRA has the advantages that it is a direct method (in contrast with iterative optimization procedures) and that it is fast (e.g. less than 2 s for the NMR data set discussed later with 16 spectra, 14 000 variables and five exponentials).

This application is called DECRA (direct exponential curve resolution algorithm) and has been applied successfully to NMR,[1,28,29] magnetic resonance (MR) images[30,31] and to determine reaction kinetics.[32,33] This paper shows a new example with NMR spectra of polymers, where five components could be resolved. Furthermore, an overview of previously done work with ultraviolet/visible (UV-vis) spectra to determine rate constants and MR images of the human brain will be given.

 

## 2. EXPERIMENTAL

### 2.1. NMR spectra of polymer solution

Approximately 5 mg of a copolymer incorporating a low-molecular-weight (low-MW) poly (dimethylsiloxane) (PDMS) segment was dissolved in dichloromethane-$d_2$. NMR spectra were acquired with a standard pulsed field gradient (PFG) probe and accessory on a Varian Inova 400 spectrometer using a stimulated echo pulse sequence[26] incorporating PFG pulses. Sixteen spectra were acquired using a gradient strength ranging from 2 to 33 G cm$^{-1}$, a diffusion time ($\Delta$) of 200 ms and a gradient pulse length of 4 ms.

Gel permeation chromatography (GPC) was used to obtain the molecular weight distribution of the polymer. A standard technique with tetrahydrofuran as the mobile phase was used to obtain the curve. Four fractions were obtained from a second run, dried with $N_2$ gas and redissolved in dichloromethane-$d_2$ for further NMR analysis. Standard proton spectra of the GPC fractions were acquired on a Varian Unity 500 spectrometer using Varian's magic angle spinning nanoprobe capable of examining as little as 20 μl of sample. A spin rate of 3 kHz was used.

### 2.2. UV-vis spectra of reaction

This subsection summarizes an extensive study where DECRA was compared with a combination of the Levenberg–Marquardt algorithm and parallel factor analysis (LM–PAR). This paper focuses on the DECRA results. For the complete report see Reference 33. In short, the two-step consecutive reaction of 3-chlorophenylhydrazonopropane dinitrile (A), an uncoupler of oxidative phosphorylation in cells, with 2-mercaptoethanol (B) forms an intermediate product (C) which is hydrolyzed in an apparently intramolecular reaction to the product 3-chlorophenylhydrazonocyanoacetamide (D) and the by-product ethylenesulfide (E). The reaction can be described as

$$\mathrm{A} + \mathrm{B} \overset{k_1}{\rightarrow} \mathrm{C} \overset{k_2}{\rightarrow} \mathrm{D} + \mathrm{E} \tag{4}$$

If 2-mercaptoethanol is present in large excess, pseudo-first-order kinetics can be assumed and the following kinetic rate equations can be used to describe the concentration profiles of A, C and D respectively:

$$C_{\mathrm{A},i} = C_{\mathrm{A},0}\mathrm{e}^{-k_1 t_i} \tag{5}$$

$$C_{\mathrm{B},i} = \frac{k_1 C_{\mathrm{A},0}}{k_2 - k_1}(\mathrm{e}^{-k_1 t_i} - \mathrm{e}^{-k_2 t_i}) \tag{6}$$

$$C_{\mathrm{D},i} = C_{\mathrm{A},0} - C_{\mathrm{A},i} - C_{\mathrm{C},i} \tag{7}$$

where $C_{\mathrm{A},i}$, $C_{\mathrm{C},i}$ and $C_{\mathrm{D},i}$ are the concentrations of species A, B and D respectively at time $t_i$, and $C_{\mathrm{A},0}$ is the initial concentration of species A at the starting point of the reaction. For equations (5–7) to be valid, only A is initially present.

The data in this paper result from monitoring this reaction by UV-vis spectroscopy. The wavenumber region used for data analysis was 300–500 nm. The components B and E do not contribute in this spectral region. As a consequence, the reactant A, intermediary C and main product D will be considered for the data analysis.

### 2.3. MR images of the human brain

MR images were acquired on a GE Signa (GE Medical Systems, Milwaukee, WI) 1·5 T whole body

 

imager employing a standard single-slice, single-echo, spin echo pulse sequence,[34] and a quadrature birdcage-style RF head coil was used to acquire axial magnetic resonance images of the brain. The image plane passed through the head of the 42-year old, healthy male volunteer at the level of the lateral ventricles. A set of 14 images were acquired in which the echo time (TE) was varied between 15 and 210 ms in 15 ms steps and the repetition time (TR) was held constant at 1000 ms. This produced an effect similar to the one described above in the PGSE NMR experiment. Here the relationship between TE and the signal of each individual component is an exponential that depends upon the component's spin–spin relaxation time ($T_2$). As TE increases, the signal from each component decreases differentially depending on the magnitude of $T_2$. From a semilog plot of signal versus TE, $T_2$ for each component may be obtained. Each 24 cm field-of-view, 5 mm slice thickness image was acquired with 256 phase-encoding steps to form a $256 \times 256$ pixel image. The motion of the volunteer was found to be minimal during the course of data collection, so no attempt was made to register the pixels within the series of correlated brain images.

### 2.4. Data analysis

For the data analysis, MATLAB software (The MathWorks, Natick, MA) was used. The computer configuration is a 266 MHz Pentium processor with 128 MB RAM.

## 3. RESULTS

### 3.1. NMR spectra of polymer solution

The following example describes the product control of a polymer reaction. The final product consists of a distribution of molecules with different molar masses. The proper product must have the low-molecular-weight PDMS chain incorporated.

The polymers in different MW classes can be separated with a diffusion experiment; see Figure 2. In order to determine whether PDMS is incorporated, one cannot simply compare plots of a 'typical' polymer peak and a 'typical' PDMS peak, since the profiles of the polymer will be linear combinations of exponentials owing to the MW distribution. Furthermore, the PDMS profile may also be a linear combination of exponentials in the case where it is present in different forms, e.g. free and incorporated into polymers of different MW classes. In order to determine the nature of incorporation of the PDMS chain in the polymer, the MW mixture needs to be resolved, for which DECRA is used. The two extremes of possible outcome for PDMS are as follows.

In the case where PDMS in not incorporated at all, the low-MW component will be separated from all the higher-MW polymers.

In the case where PDMS is incorporated completely with the high-MW component, it cannot be separated from the high-MW component. The latter is the desired outcome.

As a reference method for the separation of the different MW classes of polymers, gel permeation chromatography (GPC) was used

Figure 2 shows a stacked plot of the 16 spectra where the magnetic field gradient pulse strength ($g$) has been varied. The signal for each component decays with an exponential directly proportional to the component's diffusion coefficient in solution (or hydrodynamic size). PGSE NMR is similar to GPC for this reason. Several decay constants are seen in this data set, from the fast dichloromethane to the much slower PDMS. DECRA is applied to the data set to resolve each individual component and obtain the respective diffusion coefficients.

The resolved components are shown in Figure 3 and are ranked from fast-moving at the top to slow-moving at the bottom. The spectra are normalized in such a way as to represent accurate component composition. Aside from some visible but minor residuals, the spectral components are

 

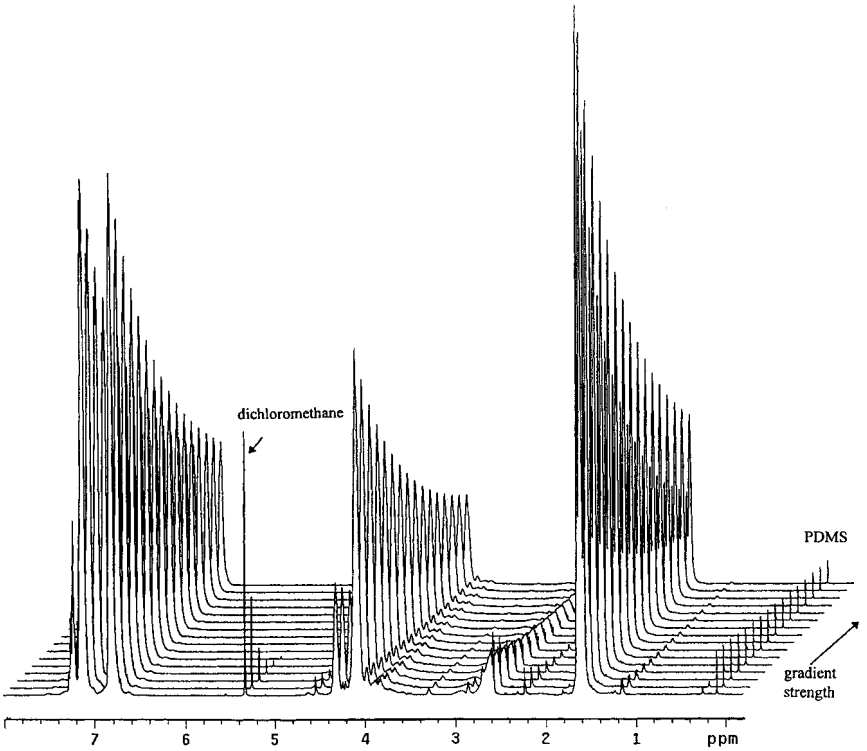


Figure 2. PGSE NMR data set resulting from diffusion experiment. Several decay constants are seen in this data set, from the fast water and dichloromethane to the much slower PDMS. The solvent is dichloromethane-$d_2$ and the temperature is 23 °C

resolved cleanly. Five exponential constants, directly related to the components' diffusion coefficients, are obtained. These results are obtained despite the severe spectral overlap of the MW components and close exponential decay rates in less than 2 s.

From the NMR data it is clear that (1) there are five primary components in the solution (including the solvents), (2) the polymeric components vary by molecular size (or MW) and are similar in chemical structure, (3) the linewidth increases with MW and (4) the PDMS, at 0·5% weight level, is incorporated into the high-MW component of the material, which shows that the product has the required properties, as stated above. If the PDMS were not incorporated, we would expect a larger diffusion coefficient, similar to the starting material, and the resonance near 0 ppm would be evident in one of the lower-MW components or as a separate component. Given the linewidth changes and similarity in molecular structure, in this case we may use the terms molecular size and molecular weight synonymously.

The resolved components are compared with extracts obtained from a GPC experiment performed on the same material (see Figure 4). The result is shown in Figure 5. The GPC curve, in Figure 4, shows several low-MW components with narrow MW distributions and high-MW components with broad MW distributions. Four fractions were obtained from the experiment and examined with NMR. The cut-off regions of the fractions are shown in Figure 4. The spectral comparisons of the resolved components from DECRA with the GPC fractions for four spectral expansions are shown in Figure 5. The DECRA-resolved spectra are very similar to the GPC fractions. The PDMS is shown to be

 

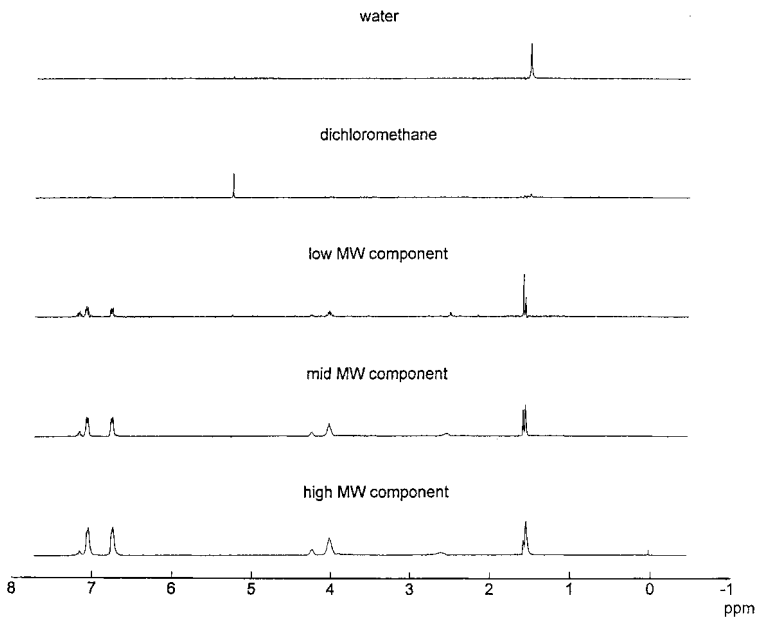


Figure 3. Five resolved components from PGSE NMR data set shown in Figure 2, ranked according to magnitude of diffusion coefficient (hydrodynamic size). The associated diffusion coefficients ($m^2\ s^{-1}$) are as follows: water, $6{\cdot}06 \times 10^{-9}$; dichloromethane-$d_2$, $3{\cdot}07 \times 10^{-9}$; low-MW polymeric component, $0{\cdot}734 \times 10^{-9}$; mid-MW polymeric component, $0{\cdot}355 \times 10^{-9}$; high-MW polymeric component, $0{\cdot}140 \times 10^{-9}$. The spectra are normalized in such a way as to represent accurate component composition

incorporated into the high-MW fraction. The spectra of fractions 3 and 4 are very similar and most closely resemble the low-MW component found by DECRA. It is clear from the GPC data that the three polymeric components and their respective exponential constants resolved by DECRA are not pure. They are actually representative averages of MW distributions. The low-MW components are most likely to be dimers, trimers, etc., having discrete diffusion coefficients very close in value. The high-MW components contain much longer chains and have broad distributions of diffusion coefficient.

This example shows that DECRA can be used for product control of polymeric reactions. The unique aspect about this data set is that we were able to resolve five exponentials in seconds with only 16 spectra, of which three were different MW classes of the polymer which have an extreme spectral overlap. There are few data analysis methods that are capable of this. Although the algorithm models the data set with discrete exponentials (and therefore discrete hydrodynamic sizes), we are still able to examine materials exhibiting broad distributions of molecular size. DECRA simply resolves the primary components, despite highly overlapped spectral features and molecular weight distributions.

### 3.2. UV-vis spectra of reaction

The kinetic properties of a chemical reaction are often of key importance. For example, in the chemical industry, rate constants of certain chemical processes are monitored to check whether a process is in or out of control. Therefore it is important that the estimations of the reaction rate constants are available rapidly in order to control the considered chemical process. The goal of this experiment was to determine whether the fast DECRA approach could be used to measure the rate

 

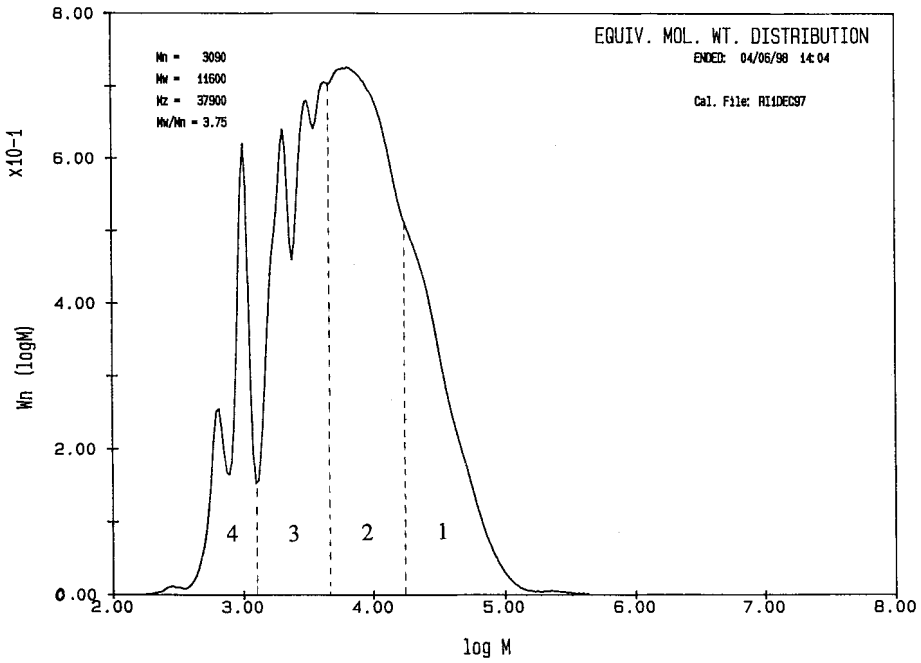


Figure 4. GPC results. The experiment was performed using THF as solvent. Four fractions were collected, dried and redissolved in dichloromethane-$d_2$

constants of a reaction. Owing to extremely high overlap of the components of interest, it is not possible to derive the rate constants from single wavenumbers. Equations (8–10) show that the concentration profiles are linear combinations of three exponential profiles:

$$C_{A,i} = f_1 e^{-k_1 t_i} \tag{8}$$

$$C_{C,i} = f_2 e^{-k_1 t_i} - f_2 e^{-k_2 t_i} \tag{9}$$

$$C_{D,i} = f_1 e^{0 t_i} - f_1 e^{-k_1 t_i} - (f_2 e^{-k_1 t_i} - f_2 e^{-k_2 t_i}) \tag{10}$$

where $f_1 = C_{A,}0$ and $f_2 = k_1\ C_{A,0}/(k_2 - k_1)$.

Note that the constant term $C_{A,0}$ in (7) is described as an exponential in (10) with a decay value of zero: $f_1 e^{0 t_i}$. This is important, since DECRA requires exponential behavior. This property of a constant has been utilized in DECRA before.[30,31]

Since the three components in the data set can be described with (linear combinations of) three exponentials, DECRA can be applied and will result in three components with exponential decay values of $k_1$, $k_2$ and zero.

The analysis of ten replicate data sets has been described extensively before.[32,33] A sample of the spectra of the averaged data set is shown in Figure 6. The data set needs to be split for DECRA. The first data set consisted of spectra 1–269, the second of spectra 2–270. The decay values derived from DECRA were 0·314 ($k_1$), 0·027 ($k_2$) and 0·000 (constant), in agreement with expectation. The spectra and contribution profiles extracted by DECRA do not represent the components of interest, since the extracted components are based on pure exponential behavior, while the components of interest are based on linear combinations of the pure exponential components. In order to calculate the actual

 

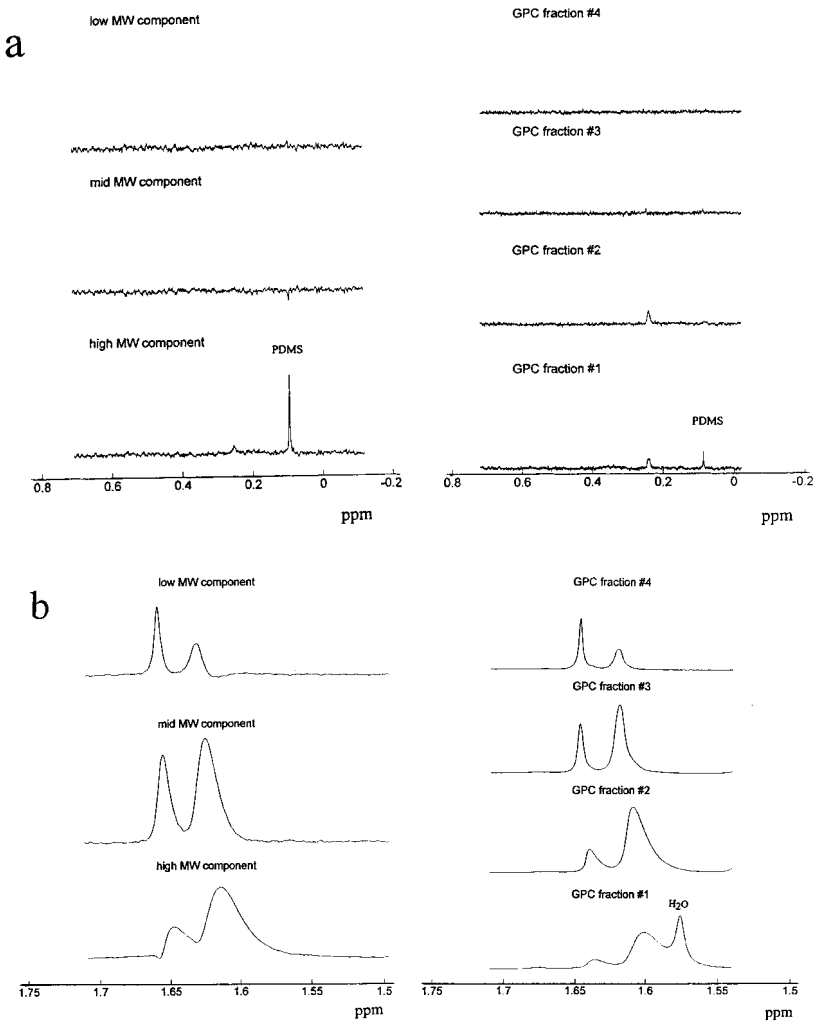


Figure 5. $^1$H spectra of GPC fractions indicated in Figure 4, compared with spectra resolved with DECRA: a, upfield region, including PDMS; b, methyl region; c, mid-spectral region; d, aromatic region. The spectra of the GPC fractions were obtained using a Varian nanoprobe capable of handling as little as 20 µl of sample. Impurities resulting from the drying step appear in the spectra of the GPC fractions and are indicated with an asterisk

components of interest, the values of $k_1$ and $k_2$ are substituted in (5)–(7), using an arbitrary value of unity for $C_{A,0}$. One has to realize that concentration values cannot be calculated unless a calibration step is involved. Each of the components' measures will have a different response factor in the spectroscopy. The contributions were scaled to reproduce the total signal (TSI) of the original spectra, using a least squares approach. As can be seen in Figure 7, TSI cannot be distinguished from the sum of the resolved curves, which clearly shows that the exponential model used to resolve this data set was correct.

The spectra associated with the contribution profiles were calculated using a least squares approach. The results are shown in Figure 8, together with reference spectra for A and D. The reference spectrum of the starting material A matches the resolved spectrum closely. Some

 

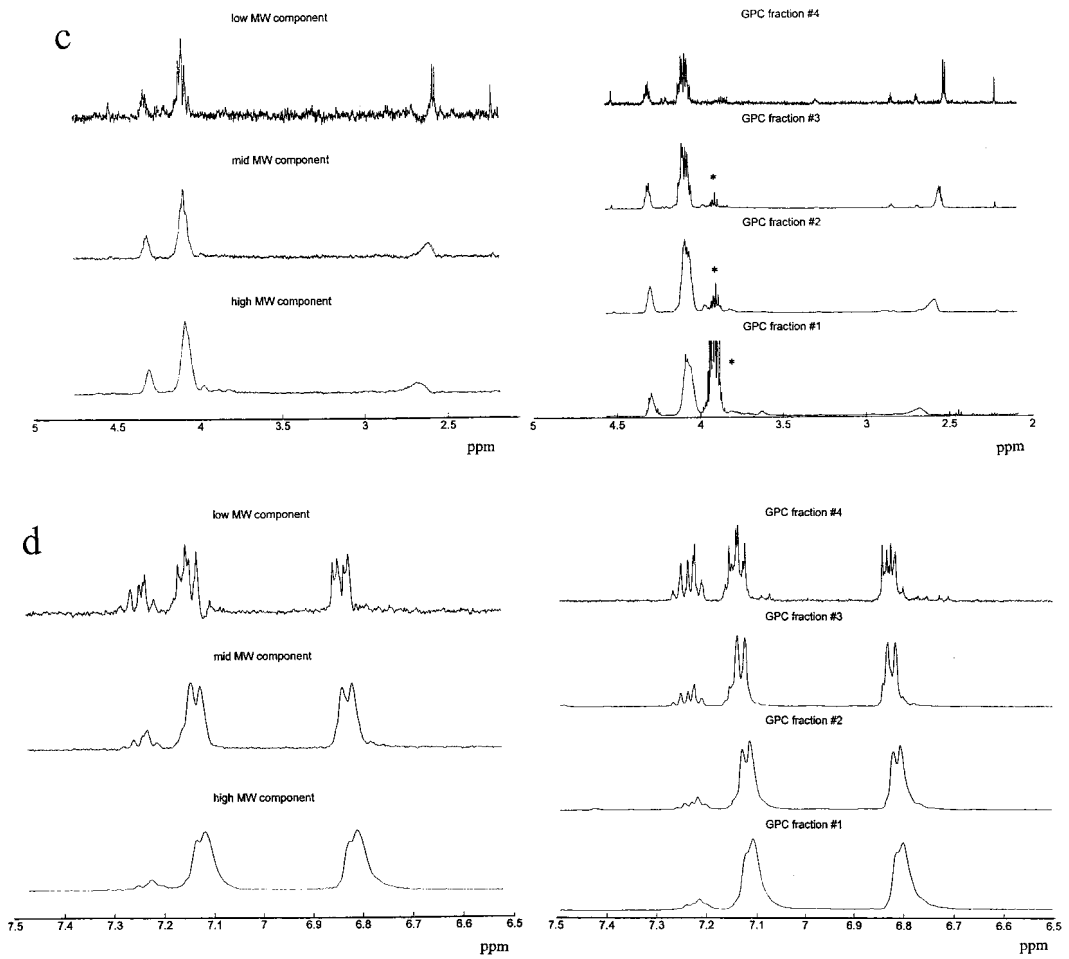


Figure 5. Continued

differences can be observed between the resolved spectrum of the end product (D) and the reference spectrum. The fit between the latter two spectra is better when using LM–PAR, but this takes hours, compared with seconds for DECRA. A reference spectrum for the intermediate product C is not available. The three resolved spectra have a very high overlap. Nevertheless, DECRA is able to resolve the data correctly.

This application of DECRA shows that it can be used as a fast method to determine rate constants from spectral data.

### 3.3. MR images of the human brain

The exponential behavior utilized to resolve the NMR data presented above can also be generated in $T_2$ experiments in magnetic resonance imaging (MRI). Different structures in the brain have an intensity that decreases by an exponential decay related to the $T_2$ properties of that structure. Generally, the results of such an experiment are 'summarized' in a single image, a $T_2$ weighted image.

 

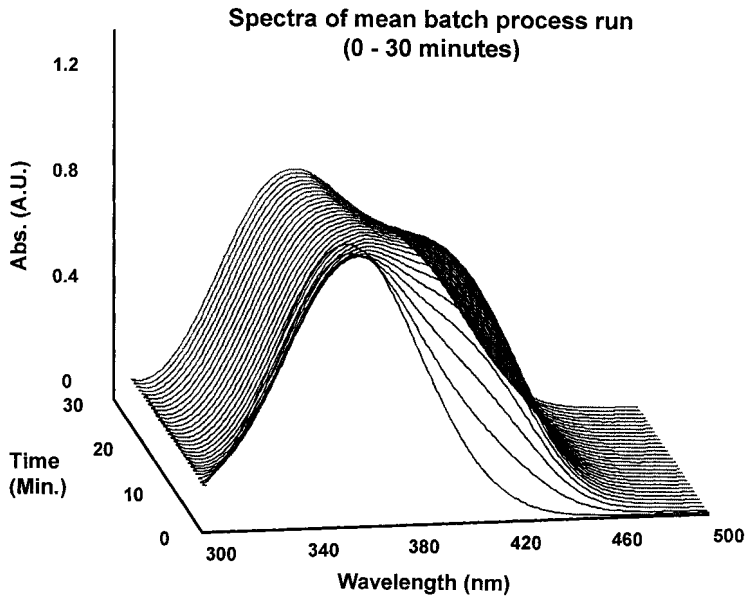


Figure 6. Sample of UV-vis spectra monitoring reaction

By resolving a series of $T_2$ MRI images into 'pure component' images, the results of the $T_2$ experiment will be the minimal number of images with the maximum information content. The increased dimensionality of the results of the experiment provides important additional information. As an analogy, one may think of a chromatogram of a sample, which shows a single summarized

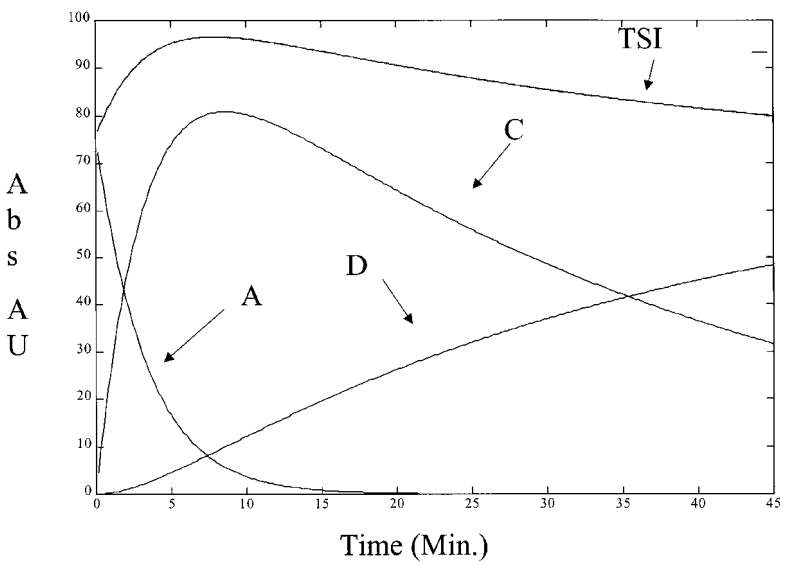


Figure 7. Extracted and scaled concentration profiles of reactant A, intermediate product C and final product D. The sum of the three curves is also plotted (—) together with TSI of the original data (.....). The two curves cannot be discriminated from each other

 

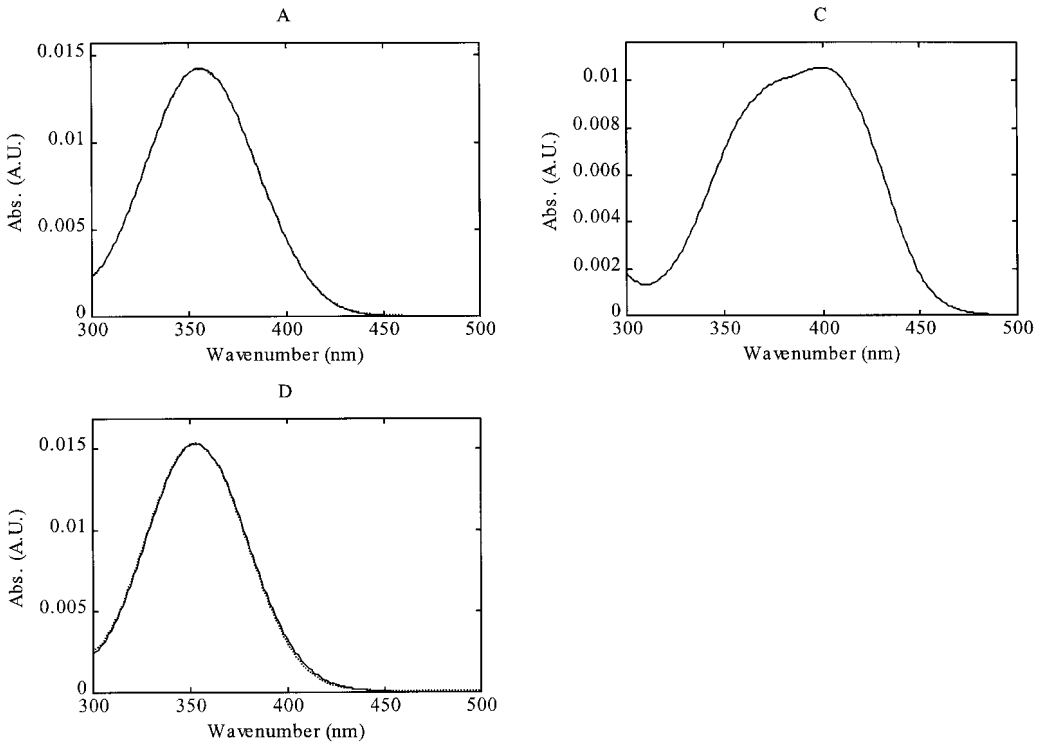


Figure 8. Resolved components. Resolved component A (—) cannot be discriminated from the reference spectrum (.....). For the intermediate product C no reference spectrum was available. The end product D (—) shows minor differences from the reference spectrum (.....)

response (such as a $T_2$ weighted image), compared with a hyphenated technique, which increases the dimensionality of chromatography, enabling the resolution of overlapping peaks (such as the resolved images).

A problem is that for MRI data each image is represented by a matrix and, as a consequence, the whole data set is represented by a series of matrices. The algorithm requires the data set to be presented in a matrix. This goal can be achieved by rearranging each MRI image into an array. The series of images can then be arranged into a matrix and can thus be treated like the spectral matrices. Successful applications of DECRA to MRI have been described.[30,31] As an example, three images out of a $T_2$ series of 14 images are shown in Figures 9(a)–(c). These images show an exponentially decaying behavior that is different for different parts of the brain. The application of DECRA to the images represented in Figures 9(a)–(c) resulted in three resolved images, which are shown in Figures 9(d)–(f). The contribution profiles (not shown) are again of clear exponential character. This shows that DECRA can be applied equally well to MR images. The analysis time is about 30–40 s on a modern PC. Although one has to be careful with the interpretation of these resolved images in biological terms, the resolved images seem to represent the following features: the first resolved image is dominated by the tissues around the skull; the second resolved image is dominated by free water, as indicated by the clear presence of the cerebrospinal fluid; and the third image seems to be dominated by water within the brain tissue.

From these results it is clear that the relatively slight differences in the continuous series of 14 MRI

 

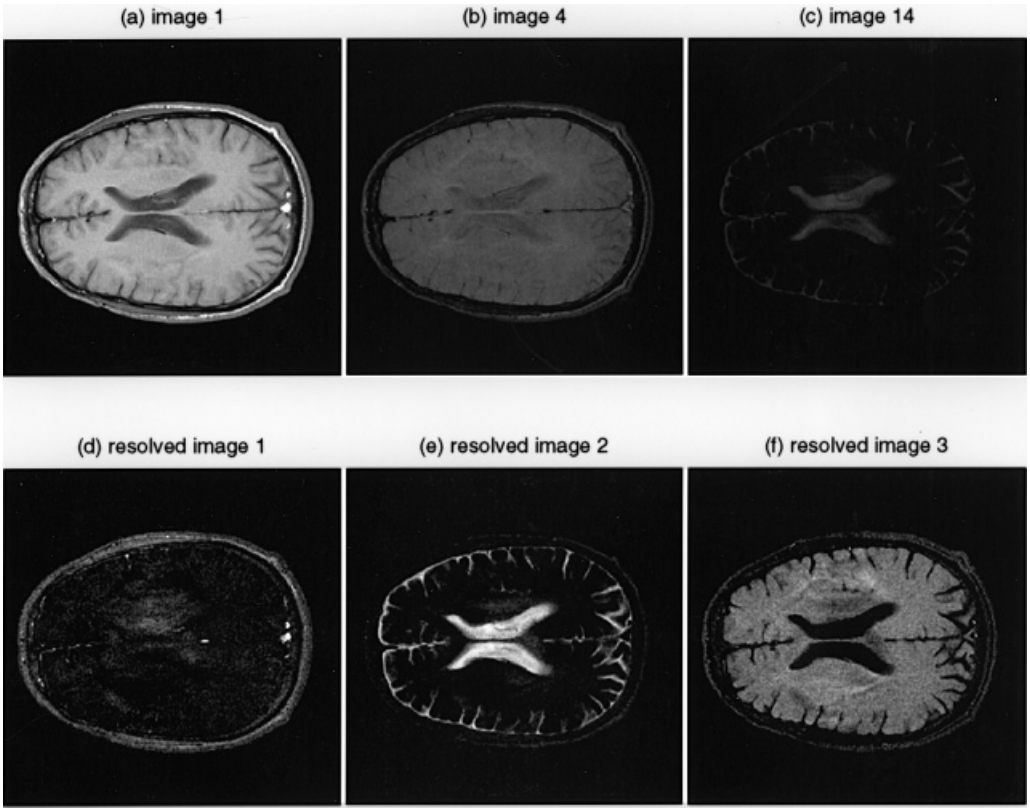


Figure 9. Images (a)–(c) represent images of the original $T_2$ data set and clearly show the decaying behavior of the intensities; images (d)–(f) represent the resolved images (reprinted from Reference 1, with permission from Elsevier Science)

images are greatly enhanced using DECRA with just three MRI images.

Next to the exponential decay profiles resulting from $T_2$ experiments, it is also possible to generate a series of images with a so-called $T_1$ experiment, where the contribution profiles can be described by the following general expression, where $x$ represents an array with equidistant increasing values:

$$a_i(1 - e^{-b_i x}) \tag{11}$$

This exponential function does not have the proportional character described above. The expression can be rewritten as

$$a_i(e^{0x} - e^{-b_i x}) \tag{12}$$

Although this is a linear combination of two exponentials, it is not possible to apply DECRA, since the rank of the data set is one. However, the solution to this problem is simple, since the decay of one exponential is known, i.e. the constant term with the decay value of zero. As a consequence, the rank of a data set can be changed simply by adding a column to the data set with a constant value. In this case one will add an extra component with a constant contribution profile, which can be ignored. The

 

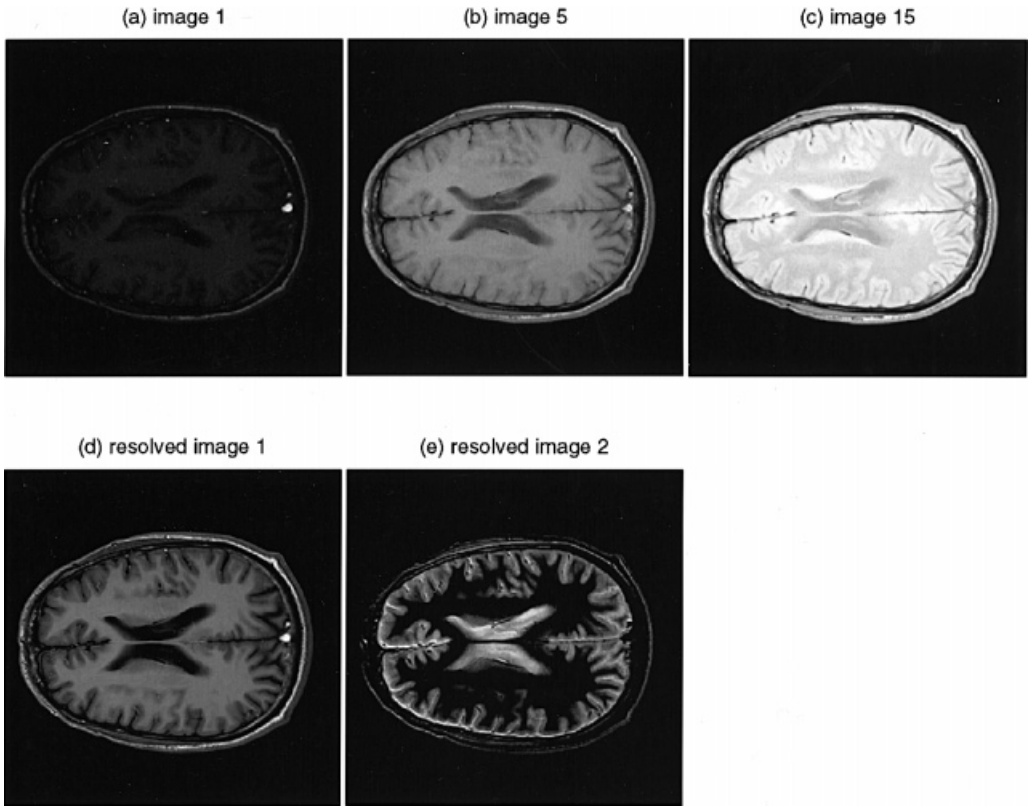


Figure 10. Images (a)–(c) represent images of the original $T_1$ data set and clearly show the exponential behavior of the intensities; images (d) and (e) represent the resolved images

other components will be expressed with the properly resolved images, but negative contribution profiles. The resolved spectra can now be used to calculate the contribution profiles using the original (i.e. without the extra column) data. Successful applications have been reported.[30,31] In Figure 10 a sample of the original images is shown along with two resolved images. The first resolved image is dominated by white matter, the second by gray matter. Again it is clear that DECRA enhances the differences in the original series of MRI images. One can expect that there are cases where this increase in the dimensionality of the results of an MRI analysis will make it possible to discriminate brain tissues (samples) in a way that cannot be distinguished with conventional techniques, similar to the enhancements that hyphenated techniques bring to conventional chromatography.

## 4. CONCLUSIONS

This paper showed the application of DECRA for very different applications. In all the cases presented, DECRA resolved the data sets successfully and at high speed. Despite the fact that exponential profiles with different decay values have high correlations, it was possible to resolve up to five components.

These results and the fact that exponential behavior is a very common feature in many processes indicate the value of DECRA as a tool to resolve data with an exponential character.

 

ACKNOWLEDGEMENTS

We thank Dr Saara M. Totterman, Director of the Magnetic Resonance Imaging Center at the University of Rochester Medical School, for providing imaging time for this study. We thank Dr Joseph P. Hornak, Center for Imaging Science at Rochester Institute of Technology, for assisting us in the imaging experiments and for providing many stimulating conversations regarding the imaging work. We thank Tom Mourey and Kim Le for the gel permeation chromatography of the samples.

## REFERENCES

1. W. Windig and B. Antalek, *Chemometrics Intell. Lab. Syst.* **46**, 207 (1999).
2. J. C. Hamilton and P. J. Gemperline, *J. Chemometrics*, **4**, 1 (1990).
3. E. R. Malinowski and D. G. Howery, *Factor Analysis in Chemistry*, 2nd edn, Krieger, Malabar, FL (1991).
4. E. R. Malinowski, *Anal. Chem.* **49**, 162 (1977).
5. E. R. Malinowski, *J. Chemometrics*, **3**, 49 (1988).
6. W. H. Lawton and E. A. Sylvestre, *Technometrics*, **13**, 617–632 (1971).
7. F. J. Knorr and J. H. Futrell, *Anal. Chem.* **51**, 1236 (1979).
8. E. R. Malinowski, *Anal. Chim. Acta*, **134**, 129 (1982).
9. K. J. Schostack and E. R. Malinowski, *Chemometrics Intell. Lab. Syst.* **6**, 21 (1989).
10. W. Windig, *Chemometrics Intell. Lab. Syst.* **36**, 3 (1997).
11. F. Cuesta Sanchez, J. Toft, B. van der Bogaert and D. L. Massart, *Anal. Chem.* **68**, 79 (1966).
12. P. J. Gemperline, *J. Chem. Info. Comput. Sci.* **34**, 206 (1984).
13. P. J. Gemperline, *Anal. Chem.* **58**, 2656 (1986).
14. B. G. M. Vandeginste, W. Derks and G. Kateman, *Anal. Chim. Acta*, **173**, 253 (1985).
15. H. Gampp, M. Maeder, C. J. Meyer and A. D. Zuberbuehler, *Talanta*, **32**, 1133 (1985).
16. M. Maeder and A. Zilian, *Chemometrics Intell. Lab. Syst.*, **3**, 205 (1988).
17. E. R. Malinowski, *J. Chemometrics*, **6**, 29 (1992).
18. E. R. Malinowski, *J. Chemometrics*, **10**, 273–279 (1996).
19. J. B. Kruskal, R. A. Harshman and M. E. Lundy, in *Multiway Data Analysis*, ed. by R. Coppi and S. Bolasco, pp. 115–122, Elsevier, Amsterdam (1989).
20. M. Kubista, *Chemometrics Intell. Lab. Syst.* **7**, 273 (1990).
21. I. Scarminio and M. Kubista, *Anal. Chem.* **65**, 409 (1993).
22. K. S. Booksh and B. R. Kowalski, *J. Chemometrics*, **8**, 287 (1994).
23. E. Sanchez and B. R. Kowalski, *Anal. Chem.* **58**, 496 (1988).
24. B. Wilson, E. Sanchez and B. R. Kowalski, *J. Chemometrics*, **3**, 493 (1989).
25. A. K. Smilde, *Chemometrics Intell. Lab. Syst.* **15**, 143 (1992).
26. P. Stilbs, *Prog. Nucl. Magn. Reson. Spectrosc.* **19**, 1 (1987).
27. P. Stilbs, K. Paulsen and P. C. Griffiths, *J. Phys. Chem.* **100**, 8180 (1996).
28. B. Antalek and W. Windig, *J. Am. Chem. Soc.* **118**, 10 331 (1996).
29. W. Windig and B. Antalek, *Chemometrics Intell. Lab. Syst.* **37**, 241 (1997).
30. W. Windig, J. P. Hornak and B. Antalek, *J. Magn. Reson.* **132**, 298 (1998).
31. B. Antalek, J. P. Hornak and W. Windig, *J. Magn. Reson.* **132**, 307 (1998).
32. S. Bijlsma, D. J. Louwerse, W. Windig and A. K. Smilde, *Anal. Chim. Acta*, **376**, 339 (1998).
33. S. Bijlsma, D. J. Louwerse and A. K. Smilde, *J. Chemometrics*, manuscript in preparation.
34. D. D. Stark and W. G. Bradley, *Magnetic Resonance Imaging*, 2nd edn, Mosby-Year Book, St Louis, MO (1992).

 